MONTANA STATE UNIVERSITY LIBRARY

Topographic controls on the leaf area index and plant functional type of a Fennoscandian tundra ecosystem

Authors: Luke Spadavecchia, Mathew Williams, Robert Bell, Paul C. Stoy, Brian Huntley, and Mark T. van Wijk

This is the peer reviewed version of the following article: see citation below, which has been published in final form at https://doi.org/10.1111/j.1365-2745.2008.01424.x. This article may be used for non-commercial purposes in accordance with Wiley Terms and Conditions for Self-Archiving.

Spadavecchia, Luke, Mathew Williams, Robert Bell, Paul C. Stoy, Brian Huntley, and Mark T. van Wijk. “Topographic Controls on the Leaf Area Index and Plant Functional Type of a Tundra Ecosystem.” Journal of Ecology 96, no. 6 (November 2008): 1238–1251. doi:10.1111/j.1365-2745.2008.01424.x.

Made available through Montana State University’s ScholarWorks
scholarworks.montana.edu

Topographic controls on the leaf area index and plant functional type of a tundra ecosystem

Luke Spadavecchia[1], Mathew Williams[1]*, Robert Bell[1], Paul C. Stoy[1], Brian Huntley[2] and Mark T. van Wijk[3]

[1]*School of GeoSciences, University of Edinburgh, Edinburgh, EH9 3JN;* [2]*Institute of Ecosystem Science, School of Biological and Biomedical Sciences, Durham University, Durham DH1 3LE, UK; and* [3]*Plant Production Systems, Wageningen University, P.O. Box 430, 6700 AK Wageningen, The Netherlands*

Summary

1. Leaf area index (LAI) is an emergent property of vascular plants closely linked to primary production and surface energy balance. LAI can vary by an order of magnitude among Arctic tundra communities and is closely associated with plant functional type.

2. We examined topographic controls on vegetation type and LAI distribution at two different scales in an Arctic tundra ecosystem in northern Sweden. 'Micro-scale' measurements were made at 0.2-m resolution over a 40 m × 40 m domain, while 'macro-scale' data were collected at approximately 10-m resolution over a 500 m × 500 m domain. Tundra LAI varied from 0.1–3.6 at the micro-scale resolution, and from 0.1–1.6 at the macro-scale resolution.

3. The correlation between dominant vascular species and LAI at the micro-scale (r^2=0.40) was greater than the correlation between dominant vegetation and LAI at the macro-scale (r^2=0.14). At the macro-scale, LAI was better explained by topographic parameters and spatial auto-correlation (pseudo r^2=0.32) than it was at the micro-scale (r^2=0.16). Exposure and elevation were significantly but weakly correlated with LAI at the micro-scale, while on the macro-scale the most significant explanatory topographic variable was elevation (r^2=0.12).

4. The distribution of plant communities at both scales was significantly associated with topography. Shrub communities, dominated by *Betula nana*, were associated with low elevation sites at both scales, while more exposed and/or high elevation sites were dominated by cryptogams.

5. *Synthesis.* Dominant vegetation, topography and LAI were linked at both scales of investigation but, for explaining LAI, topography became more important and dominant vegetation less important at the coarser scale. The explanatory power of dominant species/functional type for LAI variation was weaker at coarser scales, because communities often contained more than one functional type at 10 m resolution. The data suggest that remotely sensed topography can be combined with remotely sensed optical measurements to generate a useful tool for LAI mapping in Arctic environments.

Key-words: Arctic vegetation, geostatistics, leaf area index, multi-scale analysis, terrain indices, topography, spatial auto-regression

Introduction

The recent rate of warming in the Arctic has been two to three times the global average rate (Kattsov & Källén 2005), and may be accelerated in the future by a vegetation-albedo feedback (Chapin *et al.* 2005). Warming is likely to result in significant changes in the distribution and structure of Arctic vegetation (Sturm *et al.* 2005), with important implications for land surface properties such as the leaf area index (LAI). Predicting future changes in LAI requires a better understanding of the present distribution of Arctic vegetation, its physical and biological determinants, and the relationship between LAI and vegetation composition.

Leaf area index (LAI) is an emergent property of assemblages of vascular plants, strongly linked to albedo, primary production, evapotranspiration, surface energy balance and biogeochemical cycling (Williams *et al.* 2001; Shaver *et al.* 2007; Street *et al.* 2007). To predict the net ecosystem exchange of

CO_2 in Arctic ecosystems, it is not necessary to identify species or describe the vegeta tion, other than to estimate leaf area (Shaver *et al.* 2007). This primary importance of LAI in carbon (C) cycling is consistent with recent studies demonstrating a powerful convergence in vegetation canopy architecture, specifically between ecosystem LAI and total foliar nitrogen (N), among diverse low Arctic ecosystems (Williams & Rastetter 1999; Van Wijk *et al.* 2005). However, uncertainty in the temporal and spatial distribution of LAI (Williams & Rastetter 1999; Van Wijk *et al.* 2005) limits efforts to predict Arctic photosynthesis and C cycling at multiple spatial scales (Williams *et al.* 2001). As ner *et al.* (2003) found that spatial LAI variability in the Arctic was higher than in any of the other 15 biomes investigated. It is therefore necessary to improve understanding of the spatial distribution of Arctic LAI to estimate reliably the effects of climate change on tundra ecosystem processes.

The high variability in LAI in Arctic ecosystems is related to a high diversity in plant functional types (PFTs, e.g. deciduous or evergreen, woody or herbaceous) (Shaver & Chapin 1991) and a high degree of spatial heterogeneity in PFTs across a range of scales in low Arctic ecosystems (Williams *et al.* 2008). Vegetation assemblages are governed through the selection of individual plants through a series of environmental filters (for example, resources, conditions, disturbance), operating on a hierarchy of scales (Lavorel & Garnier 2002). The filters in Arctic ecosystems have generally been identified as primarily nutritional (Shaver *et al.* 1986; Shaver *et al.* 1992; Van Wijk *et al.* 2004), but with other important factors including tolerance to winter desiccation, soil freezing and water-logging (Shaver & Chapin 1991). The heterogeneity in vegetation suggests a highly variable distribution of environmental filters at similar scales.

In more nutrient-rich areas, the dominant PFT tends to be deciduous woody shrubs, which are the most competitive in light capture and utilisation (Shaver *et al.* 1996). Tolerance of ground freezing is required if species is to grow on the more exposed sites, which may have shallow or no snow cover. These exposed heaths tend to be dominated by evergreen dwarf shrubs. Poorly drained areas, where tolerance of waterlogged soils is required, favour sedges (Williams *et al.* 2006). The most exposed fellfields are dominated by cryptogams, with just a sparse population of vascular plants able to tolerate the shallow, dry and cold soils and exposed micro-climates.

Snow is an important determinant of vegetation cover in Arctic ecosystems. At the end of the winter, snow depths can range from a few centimetres on wind swept ridges to depths of >1 m in sheltered areas, or the lee side of slopes (Hinzman *et al.* 1996). Plants can be protected by deep snow-cover from winter desiccation and wind damage (Shaver *et al.* 1996). Soils in areas with deeper snow cover tend to be insulated from extreme low winter temperatures, thus increasing rates of nutrient cycling (Nobrega & Grogan 2007). Snowbeds also accumulate organic debris and litter, which generate nutrient additions (Sturm *et al.* 2005).

We can identify six broad controls on plant distribution and development that determine spatial patterns of LAI in Arctic ecosystems: (i) snow cover; (ii) climate, through direct effects of temperature, insolation and wind on plant development; (iii) hydrology, through the effects of soil moisture; (iv) soil/substrate variability, determining soil nutrients and soil water status; (v) biodiversity, determining the species pool and (vi) disturbance and site history, including the effects of herbivory and ecosystem management.

The first four controls are broadly related to the topography and form the focus of this study. We examine four related hypotheses to test the relative importance of topographical controls on LAI distribution in a tundra ecosystem. Our four hypotheses (H1–4) are that the primary constraint on LAI distribution is through environmental filters determined by either (H1) topographic parameters like elevation, slope and aspect, (H2) estimated landscape soil moisture, (H3) topographic exposure and associated likelihood of snow cover or (H4) derived potential insolation.

The relationships between topographic variables and LAI may vary with scale. The relationships between insolation, exposure and LAI may differ at micro-topographical (0.1–1 m) versus macro-topographical (50–100 m) scales. Hydrological variability may be important across a range of scales, from hummocks to hill slopes. There are close links among the controls, which complicates attribution. For instance, soil conditions affect infiltration, hydraulic conductivity, and plant-water availability (Darmody *et al.* 2004).

We tested the hypotheses at two different scales, defined by the horizontal resolution or 'grain' of the LAI data. The first scale test was with 0.2 m horizontal resolution LAI data within a 40 m × 40 m 'micro-scale' area, and the second was with approximately 10 m resolution LAI data within a 500 m × 500 m 'macro-scale' area. Detailed digital elevation maps (DEM) were available at both scales with appropriate resolutions. Vegetation community information was collected at both scales, allowing investigation into the connection between topography, dominant species and LAI.

This study is novel in that it uses a uniquely detailed data set, on plant community distribution, LAI and topography, to investigate vegetation-environment interactions. The data were collected at two resolutions, allowing the influences of scale and topography to be properly determined for the first time in Arctic tundra. We used statistical techniques that quantify spatial auto-correlation for appropriate fitting of geostatistical models. An additional goal of the paper was to demonstrate how topographic data can be used to improve landscape mapping of LAI, that is most typically undertaken using remote sensing of land surface reflectance (Raynolds *et al.* 2006).

Methods

STUDY SITE

The study site was located in the sub-Arctic zone of Fennoscandia, in Swedish Lapland, centred on 68 °18′54″N, 18 °50′58″E, 4.5 kilometres SSE of the Abisko Research Station. The site, hereafter referred to as the Abisko 'intensive valley' site (IV), lies within a

small (approximately 30 ha) catchment in a transition zone that intersects the local tree line (Williams *et al*. 2008). The IV has a gentle (approximately 5%) slope from south to north with an average elevation of approximately 620 m (Fig. 1). A stream runs through the centre of the area. The Abisko weather station recorded an average rainfall of 300–400 mm per annum and an average temperature of –1 °C (ASRS 2007). The hill slopes surrounding the IV reflected an extensive cover of glacial and fluvioglacial deposits, with hummocks and depressions at spatial frequencies on the order of several metres (Sonesson *et al*. 1975).

VEGETATION DESCRIPTION

A number of distinct vegetation types were observed in the IV. The willow assemblage was a shrubby riparian community dominated by grey-leaved *Salix* spp. with a *Betula nana* understorey. Dwarf birch was a community dominated by *Betula nana*, with the evergreen dwarf shrubs *Empetrum hermaphroditum* and to a lesser extent *Vaccinium vitis-idaea*. The heath community comprised the same species as observed in the dwarf birch community, but was lower-growing and dominated by *E. hermaphroditum*. The moss community was typified by *Sphagnum* spp. and characterised by the presence of *Rubus chamaemorus*, among other herb and graminoid species. The graminoid communities were assemblages of *Carex* or *Eriophorum* spp., and were associated with moist sites. The fellfield community was associated with ridges and hummock tops, comprising of a patchy (typically < 25% ground cover) cryptogam community predominantly of lichens, and a few mosses, interspersed with *B. nana*, *E. hermaphroditum*, stones and gravel.

LAI MEASUREMENTS

Measurements of LAI were conducted on a nested sampling grid at two spatial scales in the IV (Fig. 1) during the Arctic summer. All location measurements were recorded in the Universal Transverse Mercator (UTM) projection; zone 34 North, WGS 1984 datum.

Micro-scale measurements were collected from 10–31 July 2002 within a 40 m by 40 m area centred on the stream in the footslopes of the IV. The micro-scale measurements were made in nine 10 m × 10 m plots laid out on a 3 × 3 grid, with 5-m spacing between each plot (Fig. 1b). Within each of the nine micro-scale plots, indirect LAI measurements at a nominal resolution of 0.2 m were obtained by combining: (i) Normalised Difference Vegetation Index (NDVI) obtained with a Skye Instruments 2 Channel Sensor SKR 1800 (Skye Instruments, Powys, UK, channel 1 = 0.56–0.68 nm, channel 2 = 0.725–1.1 nm) with the diffuser off, held 0.9 m above the ground (referred to hereafter as 'SkyeNDVI'); and (ii) LAI estimate by a LI-COR LAI-2000 Canopy Analyzer (LI-COR, Lincoln, NE), collecting one above- and one below-canopy measurement (referred to as 'LAI-2000 LAI'). The paired LAI-2000 and NDVI measurements were conducted on a regular grid at 0.4-m intervals for each plot, giving a total of 5625 measurements. Subsequently, nine destructive harvest measurements (0.2 m × 0.2 m) of vascular plant LAI were taken for each micro-scale plot (n = 81). We used the harvest data to calibrate a model that combined the NDVI and LAI-2000 observations to generate an improved LAI estimate (van Wijk & Williams 2005). The 95% confidence interval on indirect LAI estimation varied from 0.07 to 0.2 over a range of LAI from 0–1.5 (Van Wijk & Williams 2005). Before each destructive harvest the dominant vascular plant species in each 0.2 m × 0.2 m quadrat were determined by %cover. We defined the dominant vascular species as the most abundant based on cover.

Macro-scale measurements were collected on 14–25 August 2004, in a 500 m × 500 m area encompassing the micro-scale study site. The macro-scale area was subdivided into one hundred 50 m × 50 m plots. Sixteen of these plots were further subdivided into nine intensive 10 m × 10 m plots, giving 228 measurement locations (Fig. 1). The central intensive plot corresponded with and re-sampled the micro-scale area. At the centre of each of the macro-scale sampling points, a NDVI measurement was made using the Skye sensor with its diffuser on, suspended at 3 m above ground level, resulting in a nominal resolution of approximately 10 m in diameter. Macro-scale measurements of LAI were obtained using the calibration developed from the micro-scale data (van Wijk & Williams 2005), with a detailed recalibration to account for change of sensor resolution using multi-scale nested NDVI measurements (Williams *et al*. 2008). The root-mean-square error of LAI determination at 9-m resolution was estimated at 0.08 (Williams *et al*. 2008). The location of each plot was determined to an accuracy of ±6 m using a handheld GPS (Garmine-trex). Some plots (n = 31) had a covering of birch trees over 2 m tall. It was not possible to sample NDVI effectively with the suspended Skye sensor for these plots, so they were excluded from all subsequent analyses. We consider only the remaining 197 tundra vegetation plots in this study. Based on a visual estimate of cover, we ranked the dominant three vegetation cover types, including vascular plants, mosses and lichens, for each plot. We defined the dominant vegetation based on the vegetation with the most abundant cover.

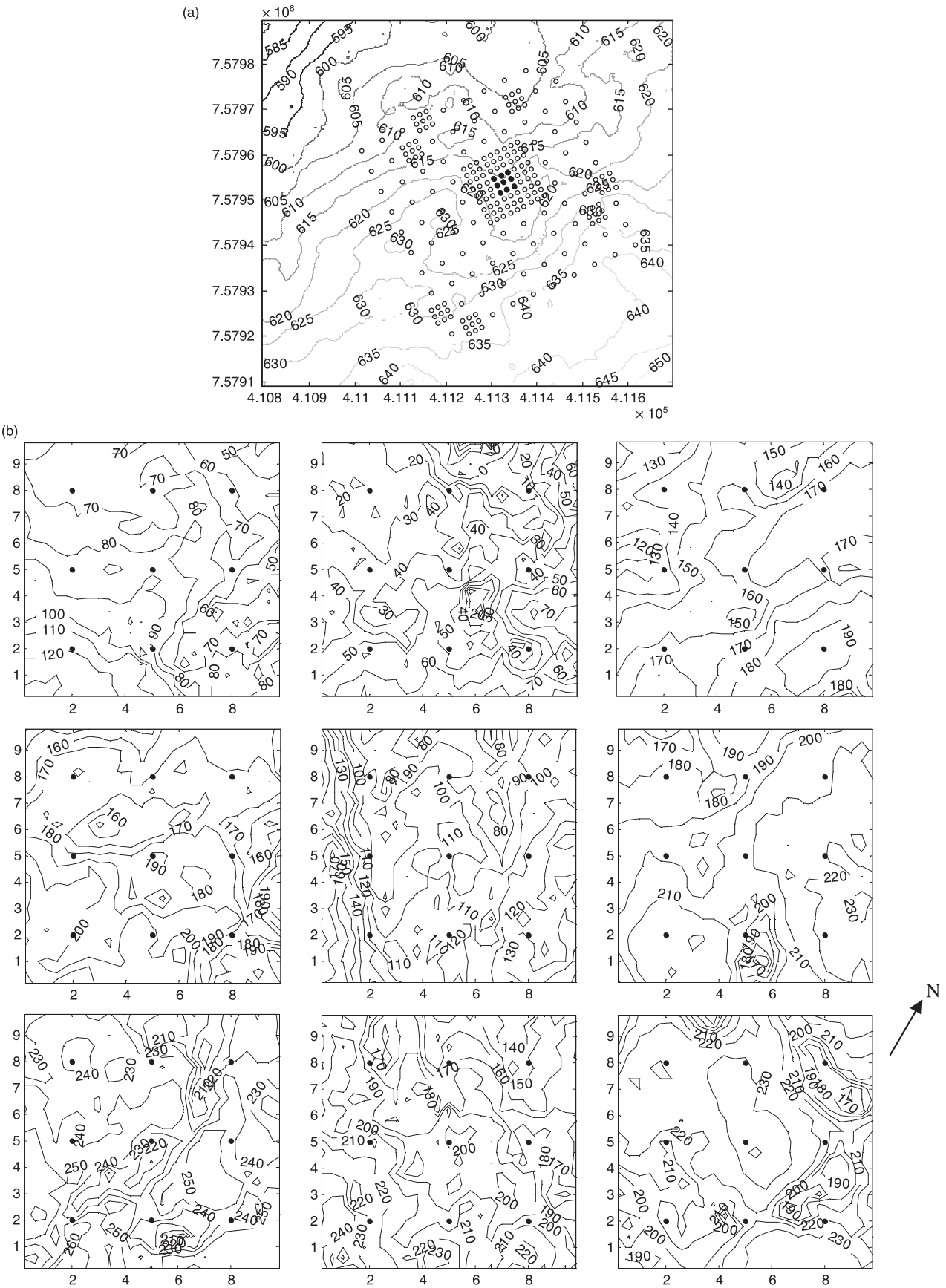
LAI surveys at the two scales were conducted 2 years apart. However, both surveys were conducted in the peak season of maximum vegetation growth, based on phenological studies at this site (Street *et al*. 2007). We thus believe that our results are robust to the difference in sampling time.

DIGITAL ELEVATION MODEL

A digital elevation model (DEM) was produced for the micro-scale site by manually surveying each of the 5625 sample locations with a level and a survey pole to record the level of the soil surface, as referenced to a zero datum at the lowest point in the plot. Measurements were collected at the same time as LAI and species data, in the period 10–31 July 2002. Instrumental precision was 0.01 m and this was the estimated error. The survey points were interpolated using inverse distance weighting (IDW) in ArcInfo (ESRI, Redlands, California) to produce a continuous surface.

The macro-scale DEM was produced from airborne LIDAR data collected by a NERC aircraft flight in July 2005 using an Optech Airborne Laser Terrain Mapper 3033 (Optech Inc., Vaughan, Ontario, Canada). The generated point cloud was gridded at 4-m resolution,

Fig. 1. (a) Digital elevation model of study site near Abisko, Sweden, showing the extent of the 'macro-scale' study area. Macro-scale measurements of LAI and vegetation type were recorded at each location marked with an open circle. The location of the 9 micro-scale plots are indicated by closed circles. The coordinates are in UTM (m), with east on the x-axis and north on the y-axis. The contours are in m above mean sea level. (b) Digital elevation model of the 'micro-scale' area and its approximate orientation. The location of the micro-scale data is indicated in the macro-scale DEM (Fig. 1a) by the filled circles. The axes are marked in m, and the contours are in cm above a local datum at approximately 615 m a.s.l. The locations of the 81 harvest plots are indicated by filled circles. The indirect LAI estimates were obtained with a 25 × 25 grid on each of the 9 subplots.


(a)
× 10^6
7.5798
7.5797
7.5796
7.5795
7.5794
7.5793
7.5792
7.5791
4.108 4.109 4.11 4.111 4.112 4.113 4.114 4.115 4.116
× 10^5
(b)
N

using minimum values of the last return pulse. Estimated elevation errors were approximately 1 m. Missing data values were interpolated using IDW, and standard pit removal procedures were undertaken in ArcInfo.

For both micro-scale and macro-scale data, a series of topographic indices were generated related to slope, aspect and surface curvature from the DEMs, by taking quadratic approximations to the first and second differentials of the surface (Evans 1980). The slope was simply the first differential of the elevation surface, while the curvature was given by the Laplacian of the DEM. Aspect was derived from directional estimates of surface gradient (Zevenbergen & Thorne 1987).

TERRAIN INDICES

The compound topographic index (CTI) was developed to summarize landscape elevs oil moisture (Beven 1977). CTI was calculated from surface drainage characteristics of the DEM, namely the upslope area (A_s) and local slope (β) (eqn 1). A_s was estimated in ArcInfo by using slope and aspect to estimate how many upstream pixels drained into a candidate pixel (Burrough *et al*. 1998). Higher scores are associated with moist sites.

$$CTI = \ln(A_s/\tan(\beta)) \quad \text{eqn 1}$$

For exposure, Toposcale 1.2 AML (Zimmerman 1999) for ArcInfo was used to estimate the TOPEX (Pyatt 1969; Wilson 1987) index. TOPEX scores were developed from the difference between a average elevation of a search window and the elevation at the central pixel of the window. The process was repeated at a number of increasing search radii, and the final TOPEX estimate was achieved by hierarchical integration over all scales (Zimmerman 1999). A high score indicates exposed positions, while negative scores indicate shelter.

Potential incoming shortwave radiation was calculated over the growing season (mid-May to mid-September), using the Shortwave AML (Kumar *et al*. 1997) for ArcInfo. The model calculated the solar geometry for each time step (30 min), taking into account the instantaneous terrain effects (slope and aspect). Shadows were projected on the surface at each time step, so terrain adjacency issues were also accounted for (Kumar *et al*. 1997). Edge effects were avoided by extending the DEM beyond the LAI data extent.

DATA TRANSFORMATION AND MODEL TESTING

Prior to analysis we ensured that the pooled LAI data approximated a normal distribution using a Box-Cox transform (Box & Cox 1964). The Box-Cox transform (Y_t) of a variable Y is given by equation 2. The power parameter λ was estimated by maximum likelihood methods.

$$Y_t = (Y^{\lambda} - 1)/\lambda \quad \text{eqn 2}$$

Ordinary least squares (OLS) regressions were fitted to the transformed data (LAI_t) to assess the significance of the derived terrain indices and models where indicated.

ORDINATION METHODS

Because of the large dataset used for the micro-scale analysis, some degree of data thinning was required for practical hypothesis testing. Topographic variables were selected on the basis of ordination, initially partitioning the parameter space using a regression tree (Breiman 1984). The regression tree method selects variables that are best able to classify the response (LAI) into distinct clusters in parameter space. The process proceeds by forward selection (binary recursive partitioning), splitting the data set using the predictor variable that explains the maximum amount of the remaining deviance in the response variable. The process results in a series of splitting rules, by which parameter space can be partitioned into ordered categories of LAI.

Trends in the parameter space were examined by principal components analysis (PCA) (Pearson 1901; Hotelling 1933). PCA re-projects the original parameter space onto an orthogonal coordinate system of principle axes, maximising the proportion of the variation in the parameter space represented by the first few dimensions. The original topographic variables were used in the analysis. The new variables created by the rotation are referred to as principal components (PCs). By examining the first three PCs on Gabriel bi-plots (Gabriel 1971), we searched for clusters of parameters that were well associated with LAI_t.

STATISTICS TO MEASURE SPATIAL DEPENDENCY

To assess the validity of OLS, we tested for auto-correlation in LAI_t using Moran's I statistic (Moran 1950). Moran's I tests for significant correlation in neighbouring points, controlled for the overall variance in the dataset. Semivariograms (Cressie 1991) were used to quantify the spatial auto-correlation structure of the data. We expressed the semivariogram in terms of a spatially continuous model to conveniently quantify spatial dependence in the data. The spherical and exponential functions which are known to be permissible were used (Christakos 1984; Mcbratney & Webster 1986). Spatial variation was characterised by the range (φ) over which auto-correlation was observed, and a 'nugget' (τ) parameter at zero separation, indicating noise or variability at smaller spatial scales than those observed.

SPATIAL REGRESSION MODELS

To account for spatial auto-correlation, we implemented spatial lattice models using maximum likelihood (ML) methods. Spatial lattice models were designed for data sampled on a grid, and include the effects of spatial auto-correlation by incorporating information on sample adjacency when fitting regressions. Adjacency was quantified using the sphere of influence (SOI) method (Jaromczyk & Toussaint 1992).

Three lattice-type models were applied to the macro-scale data: lagged-response, lagged-error, and spatial Durbin models (Haining 2003, and see Appendix S1 in Supporting Information). The lagged-response model was identical to a regular linear regression, except that the neighbouring values of LAI_t were also used in the prediction. Lagged-error models differ from OLS models by altering the error term to reflect the spatial dependence, by incorporating information about the magnitude of residuals in neighbouring points. The spatial Durbin model was the most complex model fitted, and incorporates a spatially lagged response, along with spatially lagged predictors, i.e. neighbourhood effects for all topographic variables tested, and an LAI_t auto-correlation term ρ. Details of these models can be found in the Appendix.

Lattice models were not feasible for the micro-scale data, due to computational restrictions on the 5625 data points. Instead we fitted spatial analysis of covariance (ANCOVA) models on a continuous spatial metric. The ANCOVA was fitted by ML methods, with two additional parameters (τ, ϕ) to describe the spatial error structure, as defined by the semivariogram. All statistical analyses were carried out in R version 2.4.1 (R Foundation for Statistical Computing, Vienna, Austria).

Results

The micro-scale LAI data were heavily skewed (skewness = 0.23), with most values between 0–1, but some values up to approximately 3 (Williams *et al.* 2008). The macro-scale data were more normally distributed, because of averaging occurring at a resolution of approximately 10 m (Williams *et al.* 2008). A Box–Cox transformation resulted in an normal distribution for all data, and a constant was added to the transformed LAI data to make them strictly positive. The maximum likelihood estimate of transformation parameter λ was 0.4. Unless otherwise stated, all analyses were undertaken using the transformed variable, LAI_t.

MICRO-SCALE ANALYSIS

The median untransformed LAI of the micro-scale data was 0.9, ranging from 0.1 to 3.6. Elevation ranged from 615 to 618 m, with a mean of 616.6 m. Slopes were generally on a north-westerly aspect, with 31% of all slopes facing north, 23% facing east, 14% facing south, and 32% facing west. Slopes were generally moderate, with 74% of all observations <10°, although steep inclines were observed, with a maximum of 39°. CTI was generally above zero, with a mean of 2 and a maximum of 15. PI ranged from 10 to 25 MJ m^{-2} day^{-1}, with a median of 20 MJ m^{-2} day^{-1}. Surface curvature was generally convex, with a mean curvature of 6 and a mean TOPEX of 3. TOPEX was approximately normally distributed, with a standard deviation of 68, and a range of –297 to 274. Histograms of the derived terrain indices are provided in Fig. 2.

Exploratory analysis of the micro-scale data by univariate linear regression indicated that all topographic factors and physical models for LAI_t were highly significant ($P<0.001$), with the exception of aspect ($P=0.33$) (Table 1). Despite statistical significance, all factors had low r^2 values, with a maximum of 0.05 for elevation (Table 1). A greater percentage of the variation in micro-scale LAI_t was explained by differences in the dominant species ($P<0.001$, $r^2=0.40$). However, this correlation was only for the harvest sites ($n=81$), rather than for the full micro-scale array ($n=5625$) for which topographic data were available.

Partitioning the parameter space via regression-tree analysis on the raw LAI values revealed that exposure, slope and elevation could best separate high and low LAI values (Fig. 3). Higher LAI values (mean LAI = 0.82) were associated with sheltered sites with highly negative TOPEX (< –26), low elevation sites, or areas on steeper slopes. Lower LAI values (mean LAI = 0.48) were associated with exposed topographic positions on flat surfaces at higher elevations. While indicative, this approach does not quantify the proportion of variance explained by the topographic data.

Re-projecting the parameter space via PCA similarly indicated that elevation, TOPEX and slope were strongly related to LAI_t. Principle component loadings positively associated with LAI had negative loadings of TOPEX and elevation, and positive loadings for slope (Table 2). In particular, principal component 3 (16% of variance) displayed a strong positive loading for LAI_t, and strong negative loadings for elevation and TOPEX. Comparing the first three principal components on Gabriel bi-plots (Gabriel 1971), which were split into loading and scores plots for clarity, the 0.05 and 0.95 percentiles were well separated by the coordinate rotation. On the plane of PC1 and PC3, there are clear links from LAI_t to elevation, TOPEX and slope (Fig. 4), while aspect, insolation and curvature are all orthogonal, and thus unrelated, to LAI_t.

Fitting a linear regression model to predict LAI_t from the parameters selected from ordination results indicated that all terms were highly significant ($P<0.001$, $r^2=0.11$). However, significant auto-correlation in the dataset (Moran's $I=0.68$, $P<0.0001$) indicated that robust parameter inference was not possible by simple OLS methods. A factorial ANCOVA for un-balanced sample sizes was fitted to the data (Table 3), and significant effects were identified for slope ($F=33.4$, $P<0.0001$) and TOPEX ($F=37.8$, $P<0.0001$). However, auto-correlation in the ANCOVA residuals was evident when semivariogram analysis was performed (Fig. 5).

Table 1. Linear associations between transformed micro-scale (0.2 m) LAI and terrain properties derived from a digital elevation model, ata study site near Abisko, Sweden

Micro-scale data						
Parameter	Estimate	Standard error	***t* value**	Pr(>|t|)	r^2	Kendall's τ
Elevation (m)	-2.06×10^{-091}	1.29×10^{-02}	–16.00	<0.001	0.05	–0.15
Aspect*	-2.89×10^{-02}	2.94×10^{-02}	–0.98	0.33	0.00	–0.01
Slope (°)	2.17×10^{-02}	1.48×10^{-03}	14.67	<0.001	0.04	0.13
Curvature	-3.02×10^{-04}	3.84×10^{-05}	–7.86	<0.001	0.01	–0.08
CTI†	1.61×10^{-02}	3.14×10^{-03}	5.12	<0.001	0.00	0.01
PI‡	-4.30×10^{-02}	5.61×10^{-03}	–7.69	<0.001	0.01	–0.06
TOPEX¶	-1.63×10^{-03}	1.24×10^{-04}	–13.26	<0.001	0.03	–0.13

Aspect converted to circular score ranging from 0:1 via sin(Aspect π/360).
†Compound topographic index.
‡Potential insolation over the growing season (May–September) in MJ m^{-2} d^{-1}.
§Topographic exposure index.

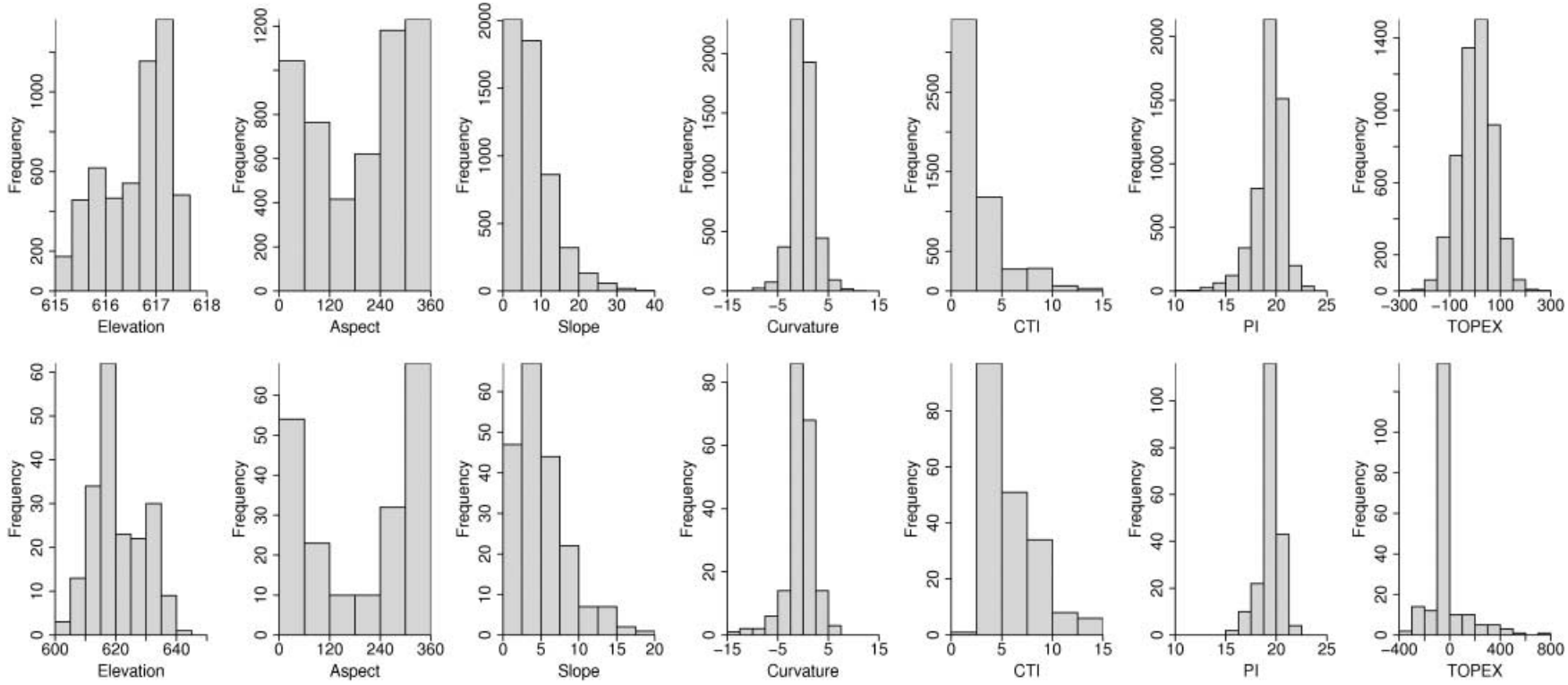


Fig.2. Histograms of DEM derived terrain indices. The upper row summarizes the micro-scale data, while the lower row contains macro-scale data. Elevations are in metres, slope and aspect are in degrees, Potential insolation (PI) is measured in MJ m^{-2} d^{-1} for the growing season, while Curvature, Compound Topographic Index (CTI) and Topographic Exposure (TOPEX) are unitless.

©2008 The Authors. Journal compilation ©2008 British Ecological Society,

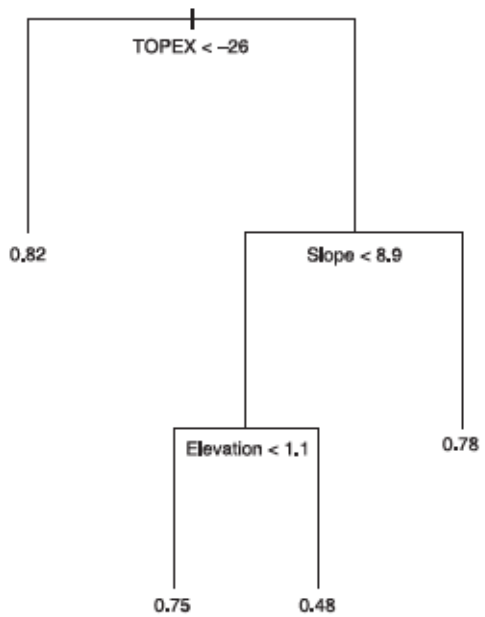


Fig. 3. Regression tree for micro-scale LAI observations. Terminal points in the tree indicate clusters in parameter space associated with high or low LAI values (mean LAI of the cluster is displayed at the terminus).

In order explicitly to treat the auto-correlation present in the data, the ANCOVA was repeated specifying exponentially structured spatial errors and spherically structured spatial errors (Fig. 5). In both cases, the fitted semivariogram models indicated auto-correlation at separation distances below 2.5 m. The models with spatial error structures both outperformed the original model (Table 4), with the additional exponential spatial structure providing the best results (Likelihood ratio = 500.0, $P < 0.0001$). After inclusion of the exponential spatial error term (Table 3) TOPEX remained highly significant ($F = 66.0$, $P < 0.0001$), but the slope effect became insignificant ($F = 2.2$, $P = 0.14$), and a significant effect of elevation was revealed ($F = 8.1$, $P < 0.01$). The spatial ANCOVA model could explain 16% of the observed variation in micro-scale LAI.

Summarising the LAI data by dominant vascular species for the 81 harvest sites indicated a strong relationship that followed expectation from plant functional types (Fig. 6). Highest LAI values were associated with deciduous shrub dominated communities (*B.nana* and *Salix spp.*) and the lowest with dwarf ericaceous shrubs (Fig. 6). The high LAI associated with deciduous species is related to their thin leaves (Van Wijk *et al.* 2005) compared to ericaceous shrubs. Thus, deciduous shrubs can produce a larger leaf area than can evergreen shrubs for the same investment of C in foliage.

When grouped by dominant species, there were close links between LAI values and elevation within the micro-scale site, with lower LAI values occurring at higher elevations. We grouped the dominant species data into the 10 m × 10 m plots ($n = 9$), and found that the mean number of 'micro-scale' dominant species per 10 m × 10 m 'macro-scale' plot was 3.2, with a range from 2–5.

MACRO-SCALE ANALYSIS

The mean LAI at the macro-scale was 0.8 with a standard deviation of 0.3 (Williams *et al.* 2008) and a range from 0.1–1.6. The smaller range of LAI at the macro-scale reflects

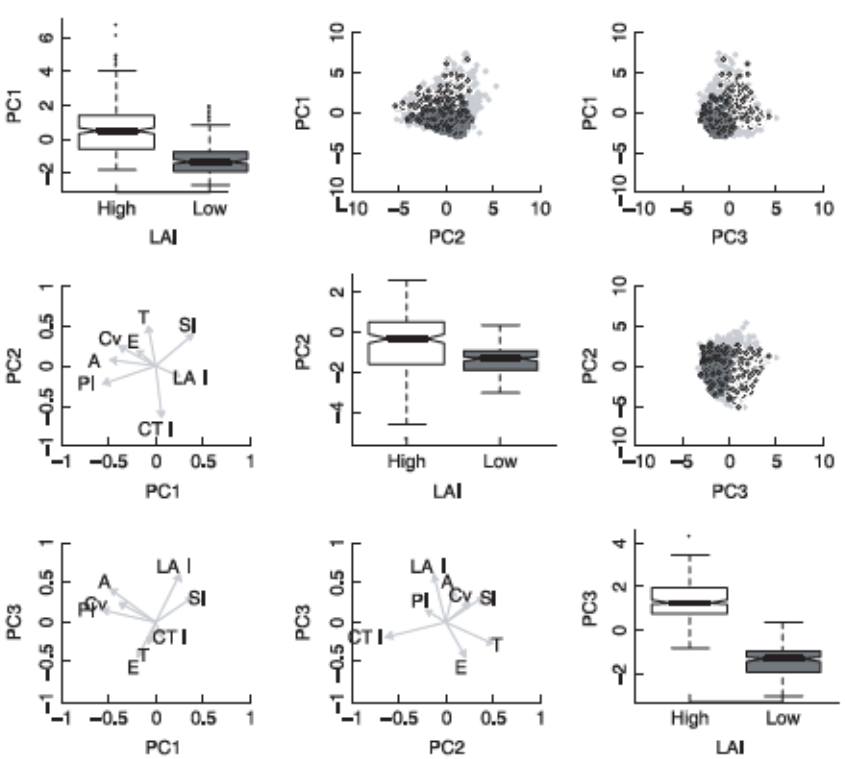


Fig. 4. Ordination matrix from principal components (PC) analysis of the micro-scale data. The matrix illustrates the relationship between the first 3 principal components of the data set, which capture 62% of the total variation. For all plots, the 95% quantiles of LAI_t are indicated in white and the 5% quantiles in dark grey. The boxplots on the diagonal show the distribution of the PC scores for the 95% and 5% LAI_t quantiles, labelled High and Low respectively. Notches indicate the non-parametric 95% confidence interval of the median. The scatter plots in the top right of the matrix show the pairwise relationship between components. The plots on the lower left of the matrix illustrate the loading of the factors for each PC. Abbreviated factor names are: LAI = transformed LAI, E = elevation, SI = slope, A = aspect, Cv = curvature, T = topographic exposure index, CTI = compound topographic index, PI = potential insolation over the growing season.

Table2. Principalcomponents(PC)analysisresultsforthemicro-scaleLAIdataset

	Loadingsbycomponent							
Factor	PC1	PC2	PC3	PC4	PC5	PC6	PC7	PC8
LAI_t	0.26	–0.13	0.59	–0.21	0.42	–0.57	0.10	–0.04
Elevation(m)	–0.20	0.20	–0.44	–0.78	–0.05	–0.33	0.04	0.01
Aspect*	–0.49	0.08	0.41	–0.27	0.16	0.33	–0.52	–0.33
Slope(°)	0.40	0.40	0.31	–0.29	–0.20	0.29	–0.17	0.59
Curvature	–0.39	0.25	0.24	0.29	–0.56	–0.54	–0.15	0.15
CTI†	0.05	–0.65	–0.19	–0.03	–0.01	–0.15	–0.61	0.39
PI‡	–0.57	–0.22	0.15	–0.04	0.22	0.16	0.46	0.56
TOPEX§	–0.09	0.50	–0.28	0.32	0.63	–0.16	–0.29	0.24
Standarddeviation	1.40	1.32	1.12	0.93	0.86	0.82	0.65	0.57
variance	0.25	0.22	0.16	0.11	0.09	0.08	0.05	0.04
Cumulativevariance	0.25	0.47	0.62	0.73	0.82	0.91	0.96	1.00

Factorloadingsforeachcomponentindicatethedirectionandmagnitudeoftheloadingofeachvariableontothecomponent.Datacaptureis indicatedbythecumulativevariance.
Aspectconvertedtocircularscorerangingfrom0:1viasin(Aspect π/360).
†Compoundtopographicindex.
‡PotentialInsolationoverthegrowingseason(May–September)inMJm $^{-2}$d $^{-1}$.
§Topographicexposureindex.

Table3. Datasummaryofdigitalelevationmapderivedtopographicindicesforthemicro-scalespatialclustersLAI $_t$valuesfromatundrasite nearAbisko,Sweden

	Highclusters		Lowclusters		ANCOVA		Spatial ANCOVA	
Parameter	Mean	SD	Mean	SD	*F*value	Pr(> *F*)	*F*value	Pr(> *F*)
LAI*	1.51	0.42	0.20	0.22				
Elevation(m)	1.45	0.65	1.85	0.50	2.41	0.12	8.12	<0.01
Slope(%)	8.99	6.29	5.84	4.05	33.39	<0.0001	2.17	0.14
TOPEX†	–7.21	76.82	22.65	54.66	37.75	<0.0001	66.03	<0.0001

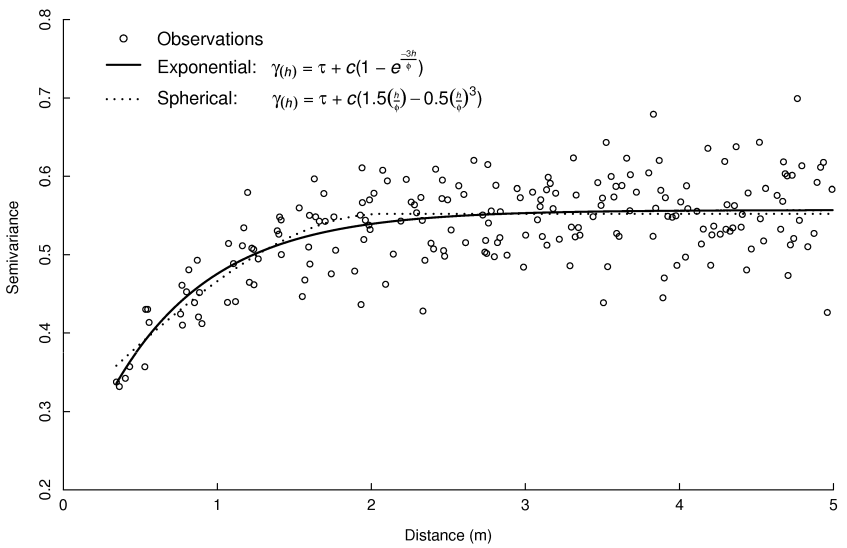


Fig.5. Semivariogram of the residuals o f the micro-scale ANCOVA. Semivariance (γ) measuresstatisticaldifferencebetweenpoints separated by a distance vector (*h*). Two models were fitted to describe the spatial structureoftheresiduals.Thesolidlineisan exponentialmodelwithintercept(τ)=0.2, andrange(φ)=2.4m.Thebrokenlineisa sphericalmodelwith τ=0.3, φ=2.3m.In bothcases,acontributionparameter(*c*)was used to scale the model. For separation distancesgreaterthan φ,thesphericalmodel takes a value equal to the sill variance (τ+ *c*).

the spatial auto-correlation of LAI of approximately 0.5–1.0mobservedatthesite(Williams*et al.*2008).Theelevation rangesampledwas604–640m,withameanof621m.Thesite wasonanorth-facingslope,with51%ofallobservationson anortherlyaspect.Slopesweremoderateonthemacro-scale, with91%ofallobservations<10°,whilethesteepestslope recordedwas18° . Most of the valley was concave, with curvatureandTOPEXscoresbelowzero.Themeancurvature

Table 4. Analysis of covariance (ANCOVA) model selection criteria for micro-scale transformed leaf area index (LAI_t) data

Model	Log likelihood	AIC	Pseudo r^2	DF
ANCOVA	−776	1565	18	6
Spatial ANCOVA 1*	−526	1069	16	8
Spatial ANCOVA 2§	−528	1071	16	8

The first model is a non-spatial analysis of covariance, fitted by maximum likelihood methods. The two spatial models add a spatially auto-correlated error function to the model, requiring an extra two degrees of freedom for the nugget (intercept τ) and (φ) range parameters. AIC is Akaike information criterion. DF is degrees of freedom.

was −0.3, while the mean TOPEX was −4. TOPEX scores were generally close to zero, indicating the macro-scale DEM with 4-m resolution was flatter than the micro-scale observations (Fig. 2). CTI scores ranged from 2 to 14, with a median value of 6. PI ranged from 15–22 MJ m^2 day^{-1}, with a median of 20 MJ m^2 day^{-1}. A summary of the DEM derived topographic indices is presented in Fig. 2.

Initial exploratory analysis of the macro-scale data by univariate linear regression indicated that only a small proportion of variation in LAI_t could be explained by topographic factors. However, there were significant relationships for elevation ($P < 0.001$, $r^2 = 0.12$), TOPEX ($P < 0.001$, $r^2 = 0.08$), aspect ($P < 0.001$, $r^2 = 0.06$) and potential insolation ($P < 0.01$, $r^2 = 0.03$) (Table 5).

Just as at the micro-scale, there was also a significant correlation between dominant vegetation type and LAI_t ($P < 0.001$, $r^2 = 0.14$). Summarizing topographic variables by dominant vegetation indicated a strong interaction between landscape level community structure and topographic position. In particular, a toposequence of community types became apparent, with a corresponding downward shift in LAI with increasing elevation (Fig. 6).

We fitted a linear mixed effects model to the macro-scale data to predict LAI_t from the full set of topographic indices and physical models, but analysis of the residuals of the fitted model showed that significant auto-correlation was present in the error term (Moran's $I = 0.14$, $P < 0.001$), indicating that OLS fitting methods were inappropriate. Residuals were found to be auto-correlated below a distance of 116 m, when an exponential auto-correlation structure was imposed upon the error term of the model. To incorporate the spatial auto-correlation structure, a series of simultaneous auto-regressive linear models were fitted to the data. Lagrange multiplier tests (Anselin 1988; Anselin & Rey 1991) indicated that fitting spatial auto-regressive models were appropriate; diagnostics for lagged-response, lagged-errors and Durbin models were all highly significant ($P < 0.0001$).

Clear improvements to the spatial regression model fit over OLS were observed for increasingly complex ML models (Table 6). The best choice of model for macro-scale LAI, as indicated by the Akaike information criterion (Akaike 1974),

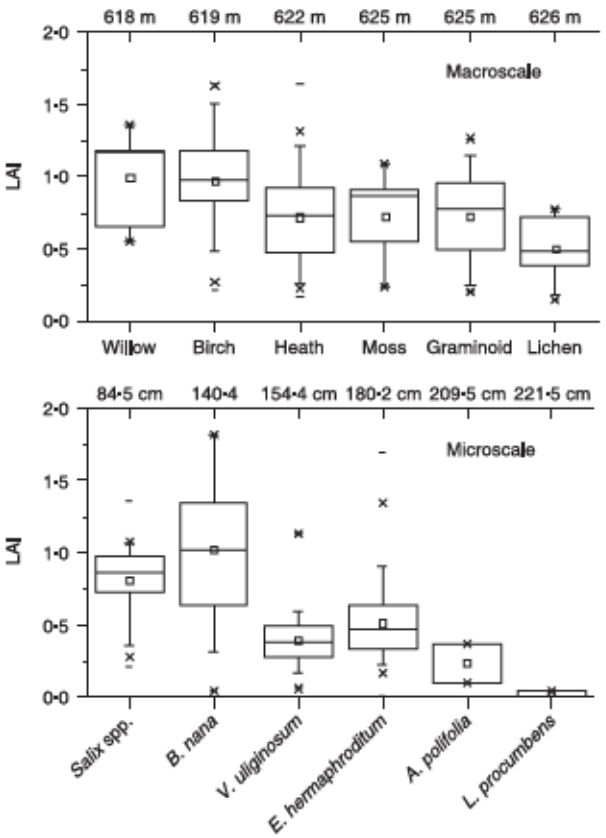


Fig. 6. Box and whisker plots of LAI by vegetation type for macro-scale (upper panel) and micro-scale (lower panel) sites sorted by elevation. In the upper panel, the macro-scale LAI was sorted by plant community type. In the lower panel the micro-scale LAI was sorted by dominant species (% cover). In both panels the data are presented in increasing order of mean elevation (a.s.l. for macro-scale, and above a zero datum at approximately 615 m a.s.l. for the micro-scale) The box extent indicates the interquartile range, while the bold central lines indicate the sample medians. The whiskers correspond to the sample 5% and 95% confidence intervals (CI). Mean LAI is indicated with an square, asterisks are the 1% and 99% CI, and indicate observed maxima and minima. *Saltx* spp, *Betula nana* and *Vaccinium uliginosum* are deciduous dwarf shrubs; *Empetrum hermaphrodittum*, *Andromeda polifolia* and *Lotseleurta Procumbens* are evergreen dwarf shrubs.

was the spatial Durbin model (pseudo $r^2 = 0.32$). An examination of the terms of the Durbin model (Table 7) indicated that the only significant local topographic term was elevation ($P < 0.001$); however, significant adjacency effects were indicated for elevation ($P < 0.01$) and PI ($P < 0.05$). Significant residual variation was also indicated by the auto-correlation parameter ρ ($P < 0.001$). The residuals of the Durbin model were not auto-correlated (Moran's $I = -0.002$, $P = 0.47$), indicating robust estimation of model parameters.

Discussion

The analyses at the macro- and micro-scales demonstrated that explicit treatments for the effects of spatial auto-correlation

Table5. Linearassociationsbetw eentr ansformedleaf area index(LAI $_t$)andindividualmacro-scaleterrainproperties,derivedfromadigital elevationmodel,fromastudysitenearAbisko,Sweden

	Macro-scaledata					
Parameter	Estimate	Std.error	*t*value	Pr(>|t|)	r^2	Kendall's τ
Elevation(m)	-1.71×10^{-02}	3.23×10^{-03}	−5.30	<0.001	0.12	−0.28
Aspect*	-3.70×10^{-01}	9.71×10^{-02}	−3.82	<0.001	0.06	−0.17
Slope(°)	8.20×10^{-03}	8.49×10^{-03}	0.97	0.35	0.00	0.07
Curvature	-1.30×10^{-02}	9.70×10^{-03}	−1.34	0.18	0.00	−0.05
CTI†	1.52×10^{-02}	1.18×10^{-02}	1.23	0.20	0.00	0.03
PI‡	-8.32×10^{-02}	2.92×10^{-02}	−2.84	<0.01	0.03	−0.15
TOPEX§	-8.00×10^{-04}	1.94×10^{-04}	−4.13	<0.001	0.08	−0.22

Aspectconvertedtocircularscoreranging from0:1viasin(Aspect π/360).
†Compoundtopographicindex.
‡PotentialInsolationoverthegrowingseason(May-September)inMJm $^{-2}$d $^{-1}$.
§Topographicexposureindex.

Table6. Linearmodelselectioncriteriaformacro-scaletransformed leafareaindex(LAI $_t$)data

Model	Loglikelihood	AIC	RMSE	Pseudo r^2	DF
OLS	−76.10	164.19	0.36	0.22	6
Laggedresponse	−69.99	153.97	0.34	0.27	7
Laggederror	−69.57	153.15	0.34	0.27	7
SpatialDurbin*	−62.75	147.50	0.33	0.32	11

TheOLSmodelisalinearregressionmodelfitbyordinaryleast squaresmethods.Theothermodelsaresimultaneousspatialauto-regressionmodelsfitbymaximumlikelihoodmethods.Thelagged responsemodeladdsaspatialinteractiontermforLAI $_t$,whilethe spatialerrormodeladdsaspatiallyinteractiveerrorterm.Thespatial Durbinmodelisthemostcomplex,addingspatialinteractionsforall predictors,andLAI $_t$.AICisAkaikeinformationcriterion.DFis degreesoffreedom.RMSEisroot-mean-square-errorofthemodel predictions.
*Laggedresponseandlaggedpredictors.

wererequiredtomakevalidinferencesregardingthedistribution of LAIunderoursamplingstrategy.Failuretotreatforthe auto-correlationinthedataledtofalseinferencesonthe significanceofeffects,mostclearlyillustratedinthe micro-scale analysis,inwhichslopeappearedtobeahighlysignificant parameter,untilauto-correlationwasaccountedfor.Similarly inthemacro-scaleanalysis,anerroneouslyhighpseudo $r^2$was arrived at before treating the analysis for spatial effects. Problemsarosebecauseoftheinflationoftheprobabilityfor committingTypeIerrorsinthepresenceofspatialauto-correlation,becauseofabiastowardsartificiallyloweringthe estimateofsamplevariance(Haining2003;Kuhn2007).For thisreason,themostusefulandvalidstatisticaloutputsofthe studywerethespatialANCOVAandthespatialDurbinmodel (Table8).

ThestatisticaltestssuggestedwecanacceptH1,thatelevation wasasignificantdeterminantofLAIatboththemacro-and micro-scales(P<0.001, P<0.01respectively,although the variance explained was low). The elevation change at the macro-scalewasanorderofmagnitudegreaterthanatthe micro-scale.Formostotherterrainindicestherewereclear andevenstrikingsimilaritiesbetweenthescales(Fig.2). Theelevationresponsewasmostclearlyobservedatthemacro-scale, and decreased in influence and significance at the micro-scale.

Increased elevation is linked with lower temperatures throughadiabaticlapserates(approximately0.6 °Cper100m). Theelevationchangeinthemacro-scalestudywas ≤40m, correspondingto≤ 0.2° Cexpecteddropinmeantemperature. Thedirecteffectsofa0.2 °Cchangeinmeantemperatureon LAIdistributionisunclear,butlikelytobesmallevenina montanesub-Arcticecosystemwithashortgrowingseason. Atthemicro-scale(elevationchangesof2–3m),theadiabatic effect on temperature would be trivial. The regression tree analysis,PCAandspatialANCOVAallconfirmedthecombined importanceofelevationandexposureinexplainingLAI variationatthemicro-scale(Table3,Figs3and4)–bothfactors arelikelytoinfluencesnowdistribution.Thusamorelikely explanationfortheelevationeffectisthroughitsinteraction withexposureindeterminingdistributionofsnowandthe acutedesiccativeandthermalstressesthataccumulatewhen thelandsurfaceisexposedtotheatmphereinwinter.

There was no significant relationship between CTI and LAIateitherthemicro-scaleorthemacro-scale,andhence werejectH2,thattheprimaryconstraintonLAIdistribution was through landscape soil moisture. We observed that drainageatthesitewascomplicatedbythestonynatureofthe substrate, a result of the intense glacial activity in the late Pleistocene.CTImaybeapoorpredictorofwatertransport throughthiscomplexsubstrate.

Therewasevidenceatthemicro-scaletosupportH3,that exposure was the dominant control on LAI, (P<0.0001), where it was observed to be the most significant factor measured,butwithlowexplanatorypower(r^2=0.03).However, therewasnosupportingevidenceforexposureeffectsatthe macro-scale,wherecalculatedTOPEXvalueswereregenerally

Table7. Spatial Durbin model of macro-scale LAI $_t$ against DEM derived terrain variables

	Macro-scaledata			
Parameter	Effect	Estimate	Likelihoodratio	Pr(>|z|)
Intercept	Intercept	9.98		
Elevation	Localeffect	-8.07×10^{-02}	11.50	<0.001
Aspect	Localeffect	-2.44×10^{-01}	3.58	0.06
TOPEX	Localeffect	-2.32×10^{-04}	1.17	0.28
PI	Localeffect	1.11×10^{-02}	0.08	0.77
Laggedelevation	Spatialinteraction	7.18×10^{-02}	8.49	<0.001
Laggedaspect	Spatialinteraction	4.43×10^{-01}	3.41	0.06
LaggedTOPEX	Spatialinteraction	-6.42×10^{-05}	0.03	0.87
LaggedPI	Spatialinteraction	-1.69×10^{-01}	6.31	<0.05
ρ	Spatialauto-correlation	0.33	11.44	<0.001

Themodelincorporateslocaleffectsoftopographyatthepredictionlocation,alongwithspatial interactionsofthesetermswithneighbouringsamples.Aneighbourhoodinteractionintheresponse(ρ)isalsoincluded.
Aspectconvertedtocircularscorerangingfrom0:1viasin(Aspect π/360).
†PotentialInsolationoverthegrowingseason(May–September)inMJm $^{-2}$d $^{-1}$.
‡Topographicexposureindex.

Table8. Asummaryofthetwokeystatisticalrelationshipsbetween LAIandtopographyidentifiedinthestudy,themethodsused,thereasonforapplyingthespecificmethod,andthekeystatisticalfinding

Relationship	Method	Reason	Keyfinding
TopographyandLAIatmacro-scale	SpatialDurbinmodel	Interactionofcontrollingfactors	pseudo r^2=0.32
Exposureandelevationeffectson LAIatmicro-scale	Spatial ANCOVA	Accountsforspatialauto-correlation	r^2=0.16

lower than at the micro-scale. TOPEX is a higher order topographic effect, derived in part from slope curvature, but a better indicator of sheltering than instantaneous curvature because it integrates enclosure over a wide distance, rather than within the narrow confines of DEM pixel adjacency. The index of exposure is likely to be an indicator of snow accumulation, or lack thereof. The significant result at the micro-scale provides support for the hypothesis that areas with snow accumulation are linked to high LAI.

H4, that short wave radiation budget was the dominant control on LAI, can be rejected; no significant effect was observed at either scale. Interestingly, PI was observed to have a negative spatial interaction with LAI at the macro-scale, indicating that an adjacent site with high solar intercept reduced the LAI at the prediction location. This may be an artefact of the dataset, or may be an outcome of the irregular hummocky topography of the site.

Overall, models of LAI distribution based on topographic parameters, and taking account of spatial auto-correlation, were able to account for 16% of the LAI variation at the micro-scale and 32% at the macro-scale. This result suggests that DEMs are useful tools in constructing maps of LAI in Arctic environments, particularly at coarser scales. LAI maps are often generated using airborne or satellite reflectance data. Our results at the macro-scale, which corresponds to the scale of high resolution satellite data, suggests that combining optical approaches for LAI determination with DEMs generated by LIDAR may result in improved regional attribution of LAI.

There were striking similarities in species/PFT-LAI patterns, and their arrangement along elevation gradients, at the different scales of investigation in this study (Fig. 6). There was a clear toposequence of PFTs at the macro-scale site, related to the correlation of elevation with LAI $_t$. On high sites, fell field communities dominated, with associated lower mean vascular LAI values. Down the elevation profile, graminoid and moss-dominated sub-Arctic meadow communities were more common, associated with relatively flat but sheltered topographic positions. Below this were heath communities, with an increasing dominance of *Betula nana* as elevation decreased, and an associated increase in mean LAI. *Salix* communities dominated on low elevation sites with steep slopes bordering the drainage channels. There was a similar toposequence of dominant vegetation at the micro-scale (Fig. 6). *Salix* spp. and *B. nana* tended to dominate at lower elevations, with dwarf shrubs as part of a lichen-dominated vegetation more common at higher sites. LAI for dominant species matched patterns and values observed at the macro-scale.

The correlation between dominant vascular species and LAI at the micro-scale (r^2=0.40) was greater than the correlation between dominant PFT and LAI at the macro-scale (r^2= 0.14). At the macro-scale, LAI was better explained by

topographic parameters and spatial auto-correlation (pseudo r^2=0.32) than it was at the micro-scale (r^2=0.16). What determined this switch in the relative importance of topography and dominant species/PFT with a change in scale? The reduction in importance of species/PFT at coarser scales was probably related to problems in defining a single PFT at 10m resolutions, because of heterogeneity in species dominance patterns. In the 10m ×10m micro-scale plots there were 2–5 different dominant species, often of different functional types, as determined from the sub-samples at 0.2-m resolution. Thus, the concept of a dominant plant functional type at 10-m resolution is questionable for this tundra ecosystem. The data suggest macro-scale communities are constructed from complex combinations of species/functional types at the micro-scale, resulting in more continuous variations and several functional types. Uncertainty in defining PFTs at 10-m resolution may explain why a continuous measure like LAI that can integrate vegetation patterns is a more effective means to identify the complex topographic and related environmental filters determining vegetation pattern at the coarser scale.

The present study did not incorporate belowground processes and plant community interaction effects, and this may account for the residual variation in the spatial patterns of LAI. The soils of Abisko have low fertility (Hinneri *et al.* 1975; Ratcliffe 2005), but their spatial variability has not been well studied. Drainage patterns, the distribution of snowbeds, and the nature of the rocky substrate probably generate a heterogeneous distribution of soil nutrients that may explain the residual variation in LAI. Factors related to site history, reindeer management and disturbance may also play an important role in the distribution of LAI. Further research into below-ground processes and community interactions is therefore likely to improve our understanding of the spatial patterning of Arctic LAI.

The results of this study should have wide applicability in explaining landscape patterns of LAI variation in tundra ecosystems across the Arctic. We can recognise the same PFTs described here in tundras elsewhere in the Arctic (Walker *et al.* 1994). These PFTs have the same general evolutionary adaptations, wherever they occur. Thus, although the species, or even in some cases the genus or family, may differ in different Arctic regions, their function is similar. As a result, we can recognise similar assemblages of PFTs occupying similar components of the tundra in response to the varying above- and below-ground conditions arising from topographic variability. Further studies on different Arctic landscapes would be valuable – for instance, focusing on older landscapes (i.e. a longer time since deglaciation) where terrain indices have been modified by a longer period of fluvial erosion, or landscapes overlying permafrost.

Conclusions

Vegetation type, topography and LAI are tightly coupled in tundra ecosystems across a broad range of scales. Examined at two different resolutions (0.2m and approximately 10m) there were striking similarities in LAI, dominant vegetation type and most terrain indices for both domains (40m ×40m, and 500m ×500m). Topographic variables explained more of the variance in LAI at the macro-scale than at the micro-scale. The explanatory power of dominant species/functional type for LAI variation was weaker at coarser scales, because communities contain more than one functional type at 10-m resolution. The explanatory power of digital elevation maps for LAI suggests that remotely sensed topography combined with remotely sensed optical measurements would be a powerful tool for LAI mapping in Arctic environments.

Acknowledgements

We are very grateful to Ana Prieto-Blanco and Mathias Disney, UCL, for generating the DEM from the aircraft data, to Lorna Street and Sven Rasmussen for assistance collecting the micro-scale dataset, to Kerry Dinsmore for assistance with the macro-scale data collection, to Gus Shaver for his support, and to the Abisko Research Station and Terry Callaghan for supporting the fieldwork. We thank two anonymous reviewers for their comments. The field work was funded by NSF grant DEB0087046 'LTER Cross-site 2000: Interactions between climate and nutrient cycling in Arctic and sub-Arctic tundra' and by the University of Edinburgh.

References

Akaike, H. (1974) A new look at statistical-model identification. *IEEE Transactions on Automatic Control*, **19**, 716–723.

Anselin, L. (1988) *Spatial Econometrics: Methods and Models*. Kluwer Academic Publishers, Dordrecht.

Anselin, L. & Rey, S. (1991) Properties of tests for spatial dependence in linear regression models. *Geographical Analysis*, **23**, 112–131.

Asner, G.P., Scurlock, J.M.O. & Hicke, J.A. (2003) Global synthesis of leaf area index observations: implications for ecological and remote sensing studies. *Global Ecology and Biogeography*, **12**, 191–205.

ASRS. (2007) Abisko scientific reasearch station weather data. Available online: URL <http://www.ans.kiruna.se/ans.htm> [Accessed 1 August 2007].

Beven, K.J. (1977) *Distributed Hydrological Modelling: Applications of the TOPMODEL Concept*. Wiley & Sons, Chichester.

Box, G.E.P. & Cox, D.R. (1964) An analysis of transformations. *Journal of the Royal Statistical Society Series B-Statistical Methodology*, **26**, 211–252.

Breiman, L. (1984) *Classification and Regression Trees*. Wadsworth International Group, Belmont.

Burrough, P.A., McDonnell, R. & Burrough, P.A. (1998) *Principles of Geographical Information Systems*. Oxford University Press, Oxford, UK.

Chapin, F.S., Sturm, M., Serreze, M.C., McFadden, J.P., Key, J.R., Lloyd, A.H. Maguire, A.D., Rupp, T.S., Lynch, A.H., Schimel, J.P., Beringer, J., Chapman, W.L., Epstein, H.E., Euskirehen, E.S., Hinzman, L.D., Jia, G., Ping, C.L., Tape, K.D., Thompson, C.D.C., Walker, D.A. & Welker, J.M. (2005) Role of land-surface changes in Arctic summer warming. *Science* **310**, 657–660.

Christakos, G. (1984) On the problem of permissible covariance and variogram models. *Water Resources Research*, **20**, 251–265.

Cressie, N.A.C. (1991) *Statistics for Spatial Data*. Wiley, Chichester.

Darmody, R.G., Thorn, C.E., Schlyter, P. & Dixon, J.C. (2004) Relationship of vegetation distribution to soil properties in Karkevagge, Swedish Lapland. *Arctic Antarctic and Alpine Research*, **36**, 21–32.

Evans, I.S. (1980) An integrated system of terrain analysis and slope mapping. *Zeitschrift für Geomorphologie, N.F., Supplementband*, **36**, 274–295.

Gabriel, K.R. (1971) Biplot graphic display of matrices with application to principal component analysis. *Biometrika*, **58**, 453–&.

Haining, R.P. (2003) *Spatial Data Analysis: Theory and Practice*. Cambridge University Press, Cambridge, UK.

Hinneri, S., Sonesson, M. & Veum, A.K. (1975) Soils of Fennoscandian IBP tundra ecosystems. *Fennoscandian Tundra Ecosystems*, Part 1 (ed. F.E. Wielkolaski), pp. 31–40. Spinger-Verlag, Berlin.

Hinzman, L.D., Kane, D.L., Benson, C.S. & Everett, K.R. (1996) Energy balance and hydrological processes in an Arctic watershed. *Landscape function and disturbance in Arctic tundra* (eds J.F. Reynolds & J.D. Tenhunen), pp. 131–154. Springer-Verlag, Berlin.

Hotelling, H. (1933) Analysis of a complex of statistical variables into principal components. *Journal of Educational Psychology*, **24**, 417–441, 498–520.
Jaromczyk, J.W. & Toussaint, G.T. (1992) Relative neighborhood graphs and their relatives. *Proceedings of the IEEE* **80**, 1502–1517.
Kattsov, V.M. & Källén, E. (2005) Future climate change: modelling and scenarios for the Arctic. *Arctic Climate Impact Assessment* (eds Symon, C., Arris, L. & Heal, B.), pp. 100–150. Cambridge University Press, Cambridge, UK.
Kuhn, I. (2007) Incorporating spatial autocorrelation may invert observed patterns. *Diversity and Distributions*, **13**, 66–69.
Kumar, L., Skidmore, A.K. & Knowles, E. (1997) Modelling topographic variation in solar radiation in a GIS environment. *International Journal of Geographical Information Science*, **11**, 475–497.
Lavorel, S. & Garnier, E. (2002) Predicting changes in community composition and ecosystem functioning from plant traits: revisiting the Holy Grail. *Functional Ecology*, **16**, 545–556.
Mcbratney, A.B. & Webster, R. (1986) Choosing functions for semi-variograms of soil properties and fitting them to sampling estimates. *Journal of Soil Science*, **37**, 617–639.
Moran, P.A.P. (1950) Notes on continuous stochastic phenomena. *Biometrika*, **37**, 17–23.
Nobrega, S. & Grogan, P. (2007) Deeper snow enhances winter respiration from both plant-associated and bulk soil carbon pools in birch hummock tundra. *Ecosystems*, **10**, 419–431.
Pearson, K. (1901) On lines and planes of closest fit to a system of points in space. *The London Dublin and Edinburgh Magazine and Journal of Science, Sixth Series*, **2**, 557–572.
Pyatt. (1969) Guide to the site types of North and Mid-Wales. Forestry Commission, Forest Record No. 69.
Ratcliffe, D. (2005) *Lapland: A Natural History*. Yale University Press, New York.
Raynolds, M.K., Walker, D.A. & Maier, H.A. (2006) NDVI patterns and phytomass distribution in the circumpolar Arctic. *Remote Sensing of Environment*, **102**, 271–281.
Shaver, G.R., Billings, W.D., Chapin, F.S. III., Giblin, A.E., Nadelhoffer, K.J., Oechel, W.C. & Rastetter, E.B. (1992) Global change and the carbon balance of Arctic ecosystems. *BioScience*, **42**, 433–441.
Shaver, G.R. & Chapin, F.S. III. (1991) Production: biomass relationships and element cycling in contrasting Arctic vegetation types. *Ecological Monographs*, **61**, 1–31.
Shaver, G.R., Chapin, F.S. III. & Gartner, B.L. (1986) Factors limiting seasonal growth and peak biomass accumulation in *Eriophorum vaginatum* in Alaskan Tussock Tundra. *Journal of Ecology*, **74**, 257–278.
Shaver, G.R., Laundre, J.A., Giblin, A.E. & Nadelhoffer, K.J. (1996) Changes in live plant biomass, primary production, and species composition along a riverside toposequence in arctic Alaska, U.S.A. *Arctic and Alpine Research*, **28**, 363–379.
Shaver, G.R., Street, L.E., Rastetter, E.B., Van Wijk, M.T. & Williams, M. (2007) Functional convergence in regulation of net CO_2 flux in heterogeneous tundra landscapes in Alaska and Sweden. *Journal of Ecology*, **95**, 802–817.
Sonesson, M., Wielgolaski, F.E. & Kallio, P. (1975) Description of Fennoscandian tundra ecosystems. *Fennoscandian Tundra Ecosystems*, Part 1 (ed. F.E. Wielkolaski), pp. 3–28. Spinger-Verlag, Berlin.
Street, L.E., Shaver, G.R., Williams, M. & Van Wijk, M.T. (2007) What is the relationship between changes in canopy leaf area and changes in photosynthetic CO2 flux in arctic ecosystems? *Journal of Ecology*, **95**, 139–150.
Sturm, M., Schimel, J., Michaelson, G., Welker, J.M., Oberbauer, S.F., Liston, G.E., Fahnestock, J. & Romanovsky, V.E. (2005) W interbiological processes could help convert arctic tundra to shrubland. *BioScience*, **55**, 17–26.
VanWijk, M.T., Clemmensen, K.E., Shaver, G.R., Williams, M., Callaghan, T.V., Chapin, F.S., Cornelissen, J.H.C., Gough, L., Hobbie, S.E., Jonasson, S., Lee, J.A., Michelsen, A., Press, M.C., Richardon, S.J. & Rueth, H. (2004) Long-term ecosystem level experiments at Toolik Lake, Alaska, and at Abisko, Northern Sweden: generalisations and differences in ecosystem and plant type responses to global change. *Global Change Biology*, **10**, 105–123.
VanWijk, M.T. & Williams, M. (2005) Optical instruments for measuring leaf area index in low vegetation: application in Arctic ecosystems. *Ecological Applications*, **15**, 1462–1470.
VanWijk, M.T., Williams, M. & Shaver, G.R. (2005) Tight couplings between leaf area index and foliage N content in arctic plant communities. *Oecologia*, **142**, 421–427.
Walker, M.D., Walker, D.A. & Auerbach, N.A. (1994) Plant communities of a tussock tundra landscape in the Brooks Range Foothills, Alaska. *Journal of Vegetation Science*, **5**, 843–866.
Williams, M., Bell, R., Spadavecchia, L., Street, L.E. & van Wijk, M.T. (2008) Upscaling leaf area index in an Arctic landscape through multi-scale observations. *Global Change Biology*, **14**, 1517–1530.
Williams, M. & Rastetter, E.B. (1999) Vegetation characteristics and primary productivity along an arctic transect: implications for scaling-up. *Journal of Ecology*, **87**, 885–898.
Williams, M., Rastetter, E.B., Shaver, G.R., Hobbie, J.E., Carpino, E. & Kwiatkowski, B.L. (2001) Primary production of an arctic watershed: an uncertainty analysis. *Ecological Applications*, **11**, 1800–1816.
Williams, M., Street, L., Wijk, M.T.V. & Shaver, G.R. (2006) Identifying differences in carbon exchange among arctic ecosystem types. *Ecosystems*, **9**, 288–304.
Wilson, J.D. (1987) Determining a TOPEX score. *Scottish Forestry*, **38**, 251–256.
Zevenbergen, L.W. & Thorne, C.R. (1987) Quantitative analysis of land surface topography. *Earth Surface Processes and Landforms*, **12**, 47–56.
Zimmerman, N. (1999) Toposcale AML. Available online: URL <http://www.wsl.ch/staff/niklaus.zimmermann/programs/aml4_1.html> [Accessed 1 August 2007].

Received 21 December 2007; accepted 1 July 2008
Handling Editor: Richard Bardgett

Supporting Information

Additional Supporting Information may be found in the online version of this article:

Appendix S1. Statistical methods for spatial analyses

Please note: Wiley-Blackwell are not responsible for the content or functionality of any supporting materials supplied by the authors. Any queries (other than missing material) should be directed to the corresponding author for the article.